

**Correlated photon emission by two excited atoms in a waveguide**Paolo Facchi,<sup>1,2</sup> Saverio Pascazio,<sup>1,3,2</sup> Francesco V. Pepe,<sup>2</sup> and Domenico Pomarico<sup>1,2</sup><sup>1</sup>*Dipartimento di Fisica and MECENAS, Università di Bari, I-70126 Bari, Italy*<sup>2</sup>*INFN, Sezione di Bari, I-70126 Bari, Italy*<sup>3</sup>*Istituto Nazionale di Ottica (INO-CNR), I-50125 Firenze, Italy*

(Received 8 October 2018; published 14 December 2018)

Systems of atoms coupled to a single or a few waveguide modes provide a test-bed for physically and practically interesting interference effects. We consider the dynamics of a pair of atoms, approximated as two-level quantum emitters, coupled to a linear guided mode. In particular, we analyze the evolution of an initial state in which both atoms are excited, which is expected to decay into an asymptotic two-photon state. We investigate the lifetime of the initial configuration and the properties of the asymptotic photon correlations, and analyze the probability that the two photons are emitted in the same or in opposite directions. We find that the ratio  $R$  between parallel and antiparallel emission probabilities is maximal when the interatomic distance is an odd multiple of a quarter wavelength of the emitted light. In such a case,  $R = 3$  in the small-coupling regime.

DOI: [10.1103/PhysRevA.98.063823](https://doi.org/10.1103/PhysRevA.98.063823)**I. INTRODUCTION**

The physics of artificial atoms embedded in one-dimensional (1D) waveguides has attracted increasing attention during the last two decades. Their interest is twofold: on one hand, 1D geometries [1,2] have unique quantum features that enable one to elucidate peculiar quantum effects in low dimensions; on the other hand, artificial dimensional reduction and related boundary conditions can profoundly modify the physical features of the systems investigated, in particular, in cavity [3–7] and circuit QED [8,9].

There are numerous experimental schemes and platforms that implement dimensional reduction and make possible the exploration and verification of photon propagation in 1D systems. Among these there are optical fibers [10,11], cold atoms [12–14], superconducting qubits [15–20], photonic crystals [21–25], and quantum dots in photonic nanowires [26,27]. The propagation of confined photons in these structures (the latter ones, in particular) is characterized by very structured energy dispersion relations and form factors, whose crucially dimension-dependent features yield novel phenomena in the decay and the dynamics [28,29].

The physics of single quantum emitters in waveguides is rather well understood [12,19,30–32]. Novel phenomena arise when two [33–43] or more [44–48] emitters are present, as photon-mediated quantum correlations start playing a crucial role, modifying dynamics and decay. In this and similar contexts, sub- and super-radiant states often emerge. However, while standard (Dicke) superradiance effects occur at light wavelengths much larger than typical interatomic distances [49,50], considering wavelengths comparable to the interatomic distance brings to light a number of interesting quantum resonance effects.

Usually, these systems are analyzed by focusing on the single-excitation sector, in which either one of the two atoms is excited or there is a photon in the waveguide. This approximation is motivated both by simplicity and by the widespread use of the rotating-wave approximation for the interaction

Hamiltonian. The double-excitation sector has been explored in less detail. This sector is made up of states in which either the two atoms are both excited and there are no photons, or one atom is excited and there is one propagating photon, or there are two photons in the waveguide. In the rotating-wave approximation, being the number of excitation conserved, the system will not leave this sector. As we shall see, a proper treatment of the system will require a suitable renormalization scheme for the vertex of the propagator.

In this article we will consider the features of spontaneous photon emission from a pair of excited atoms placed at a fixed distance along a waveguide and coupled to a single transverse field mode. The initial state is expected to relax towards an asymptotic configuration with both atoms in their ground state and two propagating photons. We will show how the emission properties are strongly influenced by interatomic distance, coupling, and excitation energy. In particular, we will focus on and compare the probabilities of parallel and antiparallel emission. If two photon detectors are placed at each end of the waveguide, only one detector will click in the case of parallel emission, detecting both photons, while both detectors will click in the antiparallel case.

In Sec. II we set up the Hamiltonian and introduce notation. In Sec. III we calculate the propagator and the decay rates. The features of the two-photon amplitude are scrutinized in Sec. IV. The two-photon correlated emission process is investigated in Sec. V. In Sec. VI we conclude and discuss our findings.

**II. THE TWO-EXCITATION SECTOR**

We shall consider a pair of distinguishable two-level systems (“atoms” in the following)  $A$  and  $B$ , embedded in a linear waveguide at a fixed distance  $d$ , and characterized by the same excitation energy  $\omega_0$  (see Fig. 1). We will assume that the atoms are both excited and are effectively coupled to a single mode of the waveguide, characterized by the dispersion

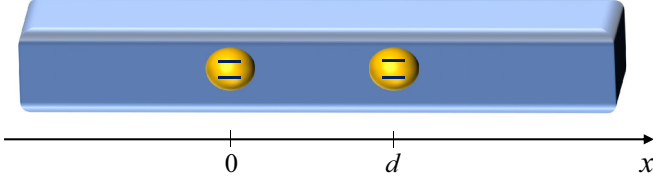


FIG. 1. Pictorial representation of two atoms  $A$  and  $B$ , modeled as two-level fixed quantum emitters, embedded in a linear waveguide at a distance  $d$  from each other. The atoms have identical excitation energy  $\omega_0$ , and we assume that the atomic transition between the excited state  $|e\rangle$  and the ground state  $|g\rangle$  is coupled only to one mode of the waveguide. In the article, we will consider the evolution from the initial double-excitation state  $|e_A, e_B\rangle$ .

relation  $\omega(k)$ . Hence, at the Fermi golden rule level, the excitation frequency  $\omega_0$  must be larger than the low-energy cutoff  $M := \min_k \omega(k)$  of the mode to enable propagation along the guide. Other modes can be neglected, either because they do not couple efficiently to the  $e \leftrightarrow g$  transition ( $g$  and  $e$  denoting the ground and excited atomic states, respectively), or because their energy cutoff is larger than  $\omega_0$ . Both conditions are easily satisfied in a lossless linear rectangular waveguide with sides  $L_y < L_z$ , where the dispersion relation of the  $\text{TE}_{1,0}$  mode reads  $\omega(k) = \sqrt{k^2 + M^2}$ , with  $M \propto L_z^{-1}$  [51], with all the other modes characterized by a larger cutoff. We will consider this dispersion relation for our analysis but will otherwise keep our discussion as general as possible.

Assuming the dipolar and rotating-wave (RW) approximations, the Hamiltonian of the system reads

$$\begin{aligned} H &= H_0 + V \\ &= \omega_0(b_A^\dagger b_A + b_B^\dagger b_B) + \int dk \omega(k) b^\dagger(k) b(k) \\ &\quad + \int dk g(k) [(b_A^\dagger + b_B^\dagger e^{ikd}) b(k) + \text{H.c.}], \end{aligned} \quad (1)$$

where  $g(k)$  is a form factor. We shall assume

$$\omega(k) = \omega(-k), \quad g(k) = g(-k). \quad (2)$$

The atomic operators  $b_{A,B}$  ( $b_{A,B}^\dagger$ ) are spin-1/2 lowering (raising) operators and  $b(k)$  ( $b^\dagger(k)$ ) are the annihilation (creation) field operators, satisfying the canonical commutation relation  $[b(k), b^\dagger(k')] = \delta(k - k')$ . The evolution determined by  $H$  preserves the total number of excitations  $\mathcal{N}$ , namely,  $[H, \mathcal{N}] = 0$ , where

$$\mathcal{N} = b_A^\dagger b_A + b_B^\dagger b_B + \int dk b^\dagger(k) b(k), \quad (3)$$

with the first two terms counting the atomic excitations and the last term counting photons. The single-excitation sector,  $\mathcal{N} = 1$ , contains, for a proper choice of the dispersion relation and for selected interatomic distances, a nontrivial atom-photon bound state [35,36], characterized by a finite probability to find the atomic excitation in a singlet or triplet state. In this article, we will consider the  $\mathcal{N} = 2$  sector. In particular, we will study the evolution of the initial state,

$$|e_A, e_B\rangle := |e_A\rangle \otimes |e_B\rangle \otimes |\text{vac}\rangle = b_A^\dagger b_B^\dagger |0\rangle, \quad (4)$$

with  $|0\rangle = |g_A\rangle \otimes |g_B\rangle \otimes |\text{vac}\rangle$  the global vacuum of the non-interacting theory, annihilated by all the  $b$  operators.

In the following it will be convenient to express the interaction Hamiltonian in terms of coupling of the symmetric and antisymmetric combinations of atomic operators:

$$V = \int dk g(k) \left( \frac{1 + e^{ikd}}{\sqrt{2}} b_+ + \frac{1 - e^{ikd}}{\sqrt{2}} b_- \right) b^\dagger(k) + \text{H.c.}, \quad (5)$$

where the new operators  $b_\pm^\dagger$  create either a triplet  $|\Psi^+\rangle$  or singlet  $|\Psi^-\rangle$  atomic Bell state from the vacuum:

$$|\Psi^\pm\rangle = b_\pm^\dagger |0\rangle = \frac{b_A^\dagger \pm b_B^\dagger}{\sqrt{2}} |0\rangle = \frac{|e_A, g_B\rangle \pm |g_A, e_B\rangle}{\sqrt{2}}. \quad (6)$$

Since  $(b_{A,B})^2 = 0$ , it is easy to check that  $b_+ b_- = 0$  and  $|e_A, e_B\rangle = \pm (b_\pm^\dagger)^2 |0\rangle$ . The pure states belonging to the  $\mathcal{N} = 2$  sector have the form

$$\begin{aligned} |\psi\rangle &= c_{AB} |e_A, e_B\rangle + \sum_{s=\pm} \int dk B_s(k) |\Psi^s; k\rangle \\ &\quad + \frac{1}{\sqrt{2}} \int dk dk' A(k, k') |k, k'\rangle, \end{aligned} \quad (7)$$

with  $|\Psi^s; k\rangle = b_s^\dagger b^\dagger(k) |0\rangle$ ,  $|k, k'\rangle = b^\dagger(k) b^\dagger(k') |0\rangle$ , and  $A(k, k') = A(k', k)$ . The coefficients must satisfy the normalization conditions

$$|c_{AB}|^2 + \sum_{s=\pm} \int dk |B_s(k)|^2 + \frac{1}{2} \int dk dk' |A(k, k')|^2 = 1. \quad (8)$$

Unlike the  $\mathcal{N} = 1$  case, the one-photon states  $|\Psi^s; k\rangle$ , directly coupled to  $|e_A, e_B\rangle$ , are also indirectly coupled to each other through the two-photon states  $|k, k'\rangle$ . Hence, the self-energy of the initial state  $|e_A, e_B\rangle$  cannot be evaluated in a closed form. However, in the following we shall discuss a partial resummation of the self-energy in order to investigate the lifetime of the initial  $|e_A, e_B\rangle$  state, the emission spectrum, and the two-photon correlations.

### III. SELF-ENERGY AND DECAY RATE OF THE DOUBLE EXCITATION

To study the evolution of the initial state  $|e_A, e_B\rangle$ , we will analyze the resolvent  $G(z) = (z - H)^{-1}$ , which determines the evolution through a Fourier-Laplace transform:

$$|\psi(t)\rangle = e^{-itH} |e_A, e_B\rangle = \frac{i}{2\pi} \int_{-\infty+ia}^{+\infty+ia} dz \frac{e^{-izt}}{z - H} |e_A, e_B\rangle, \quad (9)$$

with  $a > 0$  [3]. Since in general it is not possible to compute  $G(z)$  exactly, we consider its Dyson expansion,

$$\frac{1}{z - H} = \frac{1}{z - H_0} \sum_{n=0}^{\infty} \left( V \frac{1}{z - H_0} \right)^n, \quad (10)$$

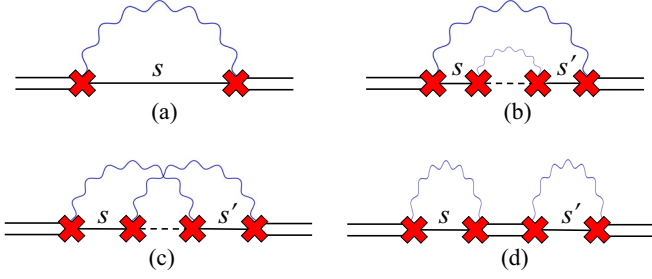


FIG. 2. Contributions of order  $V^2$  [diagram (a)] and  $V^4$  [diagrams (b), (c), and (d)] to the double-excitation propagator  $G_2(z)$  [Eq. (17)]. The diagrams (a), (b), and (c), without external legs, represent the  $O(V^4)$  contributions to the self-energy  $\Sigma_2(z)$ . The wavy lines represent photons; the double horizontal line represents the free propagator  $G_2^{(0)}(z)$  in (11); the single horizontal line with a wavy line represents the free propagator (12) of  $|\Psi^s; k\rangle$ , namely, the state with one photon and a single atomic excitation with sign  $s$ ; and the dashed line with two wavy lines represents the free propagator  $G_1^{(0)}(z, k)$  in (13). The crosses represent one of the vertices  $v_s(k)$  in (14)–(16). Processes (b) and (c) preserve the sign  $s$  (i.e.,  $s' = s$ ), while in diagram (c) the relative sign of  $s$  and  $s'$  is arbitrary.

and sum the relevant diagrams. The basic building blocks of the matrix elements of the expanded resolvent (10) are given by the free propagators

$$\langle e_A, e_B | \frac{1}{z - H_0} | e_A, e_B \rangle = \frac{1}{z - 2\omega_0} = G_2^{(0)}(z), \quad (11)$$

$$\langle \Psi^{s'}; k' | \frac{1}{z - H_0} | \Psi^s; k \rangle = G_1^{(0)}(z, k) \delta_{s,s'} \delta(k - k'),$$

$$G_1^{(0)}(z, k) = \frac{1}{z - \omega_0 - \omega(k)}, \quad (12)$$

$$\langle k'_1, k'_2 | \frac{1}{z - H_0} | k_1, k_2 \rangle = G_0^{(0)}(z, k_1, k_2) [\delta(k_1 - k'_1) \delta(k_2 - k'_2) + \delta(k_1 - k'_2) \delta(k_2 - k'_1)],$$

$$G_0^{(0)}(z, k_1, k_2) = \frac{1}{z - \omega(k_1) - \omega(k_2)}, \quad (13)$$

and by the interaction vertices

$$\langle \Psi^s; k | V | e_A, e_B \rangle = s v_s(k), \quad (14)$$

$$\langle k_1, k_2 | V | \Psi^s; k \rangle = v_s(k_1) \delta(k_2 - k) + v_s(k_2) \delta(k_1 - k), \quad (15)$$

$$v_s(k) = g(k) \frac{1 + s e^{ikd}}{\sqrt{2}}, \quad (16)$$

with  $s = \pm 1$ . Since the interaction Hamiltonian is off-diagonal, no  $O(V)$  terms appear in the decomposition of the propagator,

$$G_2(z) = \langle e_A, e_B | G(z) | e_A, e_B \rangle = \frac{1}{z - 2\omega_0 - \Sigma_2(z)}, \quad (17)$$

where  $\Sigma_2(z)$  is the self-energy of  $|e_A, e_B\rangle$ . The smallest-order contribution to (17) comes from the process of emission and reabsorption of a photon through an intermediate state  $|\Psi^s, k\rangle$ . In this process, represented in Fig. 2(a), it is clear from (12) that the atomic excitation cannot switch its sign  $s$  during the

intermediate free evolution, before the photon is reabsorbed. Transitions can generally occur only in higher-order diagrams, such as the  $O(V^4)$  terms in Figs. 2(b)–2(d). However, a diagram in which a photon is emitted and then reabsorbed takes the general form

$$\int dk g^2(k) \frac{(1 + s' e^{-ikd})(1 + s e^{ikd})}{2} \Phi_{ss'}(z, \omega(k)), \quad (18)$$

where  $s$  ( $s'$ ) is the sign of the atomic excitation attached to the emission (absorption) vertex, and the function  $\Phi$  is related to the particular structure of the diagram. Since we have assumed that both the dispersion relation and the form factor are even functions, only terms with  $s = s'$  survive integration over  $k$  and contribute, for instance, to the diagrams in Figs. 2(b) and 2(c); no constraint on the relative sign exists, instead, for the diagram (d).

The diagrams (b) and (c) in Fig. 2 are both contributions of order  $V^4$  to the self-energy of  $|e_A, e_B\rangle$ , but they qualitatively differ. In (b), the emission and reabsorption of a second photon is dressing the intermediate one-excitation propagator, while this is not the case in (c), where, since the first emitted photon is absorbed before the second one, two photon lines cross. Diagrams with crossings can be interpreted as a renormalization of the vertex between the double-excitation state  $|e_A, e_B\rangle$  and the states  $|\Psi^s; k\rangle$ . Notice that since we consider the dynamics in the  $\mathcal{N} = 2$  sector, where at most two photons can be present in an intermediate state, each photon line can cross at most two other lines before being reabsorbed. The self-energy appearing in (17), containing the sum of all the intermediate diagrams between the two double-excitation states, can be resummed as

$$\Sigma_2(z) = \sum_{s=\pm} \int dk g^2(k) \frac{(1 + X_s(k, z))(1 + s \cos(kd))}{z - \omega_0 - \omega(k) - \Sigma_s(z - \omega(k))}, \quad (19)$$

where  $\Sigma_s$  is the self-energy of the one-excitation state  $|\Psi^s\rangle$ ,

$$\Sigma_s(z) = \int dk g^2(k) \frac{1 + s \cos(kd)}{z - \omega(k)}. \quad (20)$$

Observe that in Eq. (19), the argument of  $\Sigma_s$  is shifted by the energy  $\omega(k)$  of the additional propagating photon [35], and notice that  $\Sigma_s(z - \omega(k))$  does *not* coincide with the self-energy function of  $|\Psi^s; k\rangle$ . The vertex renormalization  $X_s$  is implicitly defined by the integral equation

$$X_s(k, z) = \int dq g^2(q) \frac{(1 + X_s(q, z))(1 + s \cos(qd))}{z - \omega_0 - \omega(k) - \Sigma_s(z - \omega(k))} \times \frac{1}{z - \omega(q) - \omega(k)}. \quad (21)$$

The renormalization of the propagator  $G_2(z)$  is graphically represented in Fig. 3.

The evaluation of the renormalized vertex requires an approximation procedure that will be detailed in the next section, where it will be crucial for the consistent evaluation of the two-photon amplitude and spectrum.

In order to characterize the lifetime of the double excitation, it is sufficient to consider the lowest order of the self-energy by neglecting  $X_s(k, z)$  and  $\Sigma_s(z - \omega(k))$  in its integral

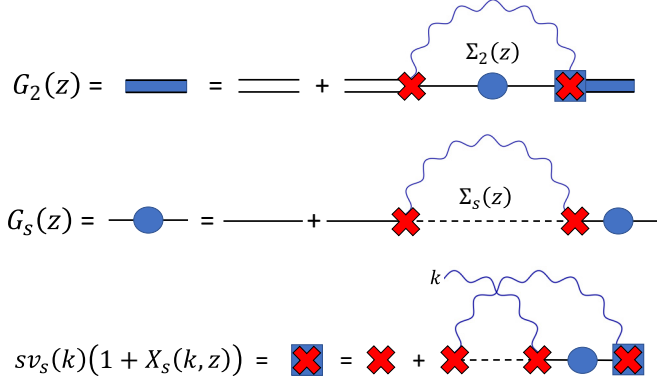


FIG. 3. Renormalization scheme for the two-excitation state propagator  $G_2(z)$ .

expression (19), namely,

$$\Sigma_2^{(2)}(z) = \sum_{s=\pm} \Sigma_s(z - \omega_0) = \int dk \frac{2g^2(k)}{z - \omega_0 - \omega(k)}. \quad (22)$$

By evaluating the self-energy on shell  $\Sigma_2(2\omega_0)$ , in the propagator (17) we can infer, as a first approximation, that the lifetime of the double excitation,

$$\tau_2 \simeq -(2\text{Im}[\Sigma_2^{(2)}(2\omega_0 + i0)])^{-1}, \quad (23)$$

is half the lifetime of a single *isolated* excited atom, independently of the interatomic distance. It is evident from (22) that the lowest-order contribution to the lifetime of  $|e_A, e_B\rangle$  is insensitive to the interatomic distance, and *a fortiori*, to the existence of resonant bound states in the  $\mathcal{N} = 1$  sector. This result is physically in accord with the fact that photon exchanges between the two atoms are neglected at  $O(V^2)$  of the self-energy and is consistent with the oscillating behavior of the lifetimes of  $|\Psi^\pm\rangle$  in the one-excitation sector [35]: the state  $|e_A, e_B\rangle$  has two decay modes, and when one of them is close to a resonant bound state, the antiresonant mode has twice the lifetime of an isolated atom. The effects related to interatomic distance will emerge in the analysis of the photon pair emitted by the double-excitation state, which is the topic of the following section.

Finally, it is worth noticing that since the self-energy functions  $\Sigma_s(z)$  in (20) are characterized by a branch cut along the half line  $[M, \infty)$  on the real axis, the  $O(V^2)$  contribution to the self-energy (22) has a cut in correspondence of  $[M + \omega_0, \infty)$ . However, considering the exact expression (19), one finds that the branch cut of the self-energy [and of the propagator  $G_2(z)$  as well] actually starts from  $2M$ . This result, as we will show in the following, is consistent with the integrability of the asymptotic two-photon distribution.

#### IV. TWO-PHOTON AMPLITUDE

One of the most interesting features of the evolution dynamics of the initial state  $|e_A, e_B\rangle$  under the action of the Hamiltonian (1) are correlations and interference effects involving the emission of two photons. Unlike the lifetime of the initial state, such effects are deeply influenced by the

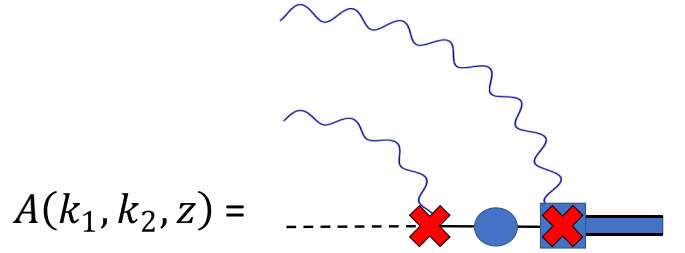


FIG. 4. Diagrammatic representation of the two-photon amplitude  $A(k_1, k_2, z) = \langle k_1, k_2 | (z - H)^{-1} | e_A, e_B \rangle$ . The dressed propagators and the dressed vertex are defined in Eqs. (19)–(21) and represented in Fig. 3.

existence of resonant bound states in the  $\mathcal{N} = 1$  sector. The properties of the two-photon amplitude at a generic time  $t$ ,

$$A(k_1, k_2, t) = \langle k_1, k_2 | e^{-itH} | e_A, e_B \rangle, \quad (24)$$

are determined through Eq. (9) by its representation in the energy domain, which, by following the same resummation procedure as for the self-energy (19), reads

$$A(k_1, k_2, z) = \langle k_1, k_2 | \frac{1}{z - H} | e_A, e_B \rangle = \frac{A(k_1, k_2, z)}{z - \omega(k_1) - \omega(k_2)}, \quad (25)$$

with

$$A(k_1, k_2, z) = \sum_{s=\pm} \frac{sv_s(k_1)v_s(k_2)}{z - 2\omega_0 - \Sigma_2(z)} \times \sum_{j=1,2} \frac{1 + X_s(k_j, z)}{z - \omega_0 - \omega(k_j) - \Sigma_s(z - \omega(k_j))}. \quad (26)$$

See the Feynman diagrams in Fig. 4.

In order to characterize the properties of the two-photon amplitude, we will specialize our analysis to the case of a pair of atoms coupled to a massive guided mode, characterized by the following dispersion relation and form factor [35]:

$$\omega(k) = \sqrt{k^2 + M^2}, \quad g(k) = \frac{\lambda}{\sqrt[4]{k^2 + M^2}}, \quad (27)$$

where the units are chosen in a way that the speed of light in the waveguide is equal to 1. We also introduce for convenience the on-shell quantities  $k_0 > 0$ ,  $c_0$ , and  $g_0$ :

$$\omega(k_0) = \omega_0, \quad c_0 = \left. \frac{d\omega}{dk} \right|_{k=k_0}, \quad g_0 = \frac{\lambda}{\sqrt{\omega_0}}. \quad (28)$$

Since the relevance of the one-excitation self-energy functions  $\Sigma_s(z)$ , with  $s = \pm$ , is manifest in Eqs. (25) and (26), let us review their properties before discussing the two-photon amplitude. In the case (27), the self-energy can be analytically evaluated for  $\text{Re}(z) > 0$ , where it reads [35]

$$\Sigma_s(z) = \frac{2\lambda^2}{\sqrt{z^2 - M^2}} \left[ [1 + s\xi(z)] \ln \frac{z + \sqrt{z^2 - M^2}}{M} - i\pi(1 + se^{i\sqrt{z^2 - M^2}d}) \right], \quad (29)$$

with  $\xi(z) = O(e^{-Md})$  a real-valued function for real  $z$ . Notice the square-root divergence at the branching point  $z = M$ , which depends on the diverging density of states close to the threshold  $M$  for photon propagation. The existence of bound states for special values of the interatomic distance is related to the oscillating behavior of the imaginary part of (29). In particular, considering the lowest order in  $\lambda$  and neglecting the  $O(e^{-Md})$  corrections, the energy shift and decay rate of  $|\Psi^s\rangle$  can be written as

$$\delta_s = \text{Re}[\Sigma_s(\omega_0 + i0)] \simeq \delta_0 + 2\pi s \frac{g_0^2}{c_0} \sin(k_0 d), \quad (30)$$

$$\gamma_s = -2\text{Im}[\Sigma_s(\omega_0 + i0)] = 4\pi s \frac{g_0^2}{c_0} [1 + s \cos(k_0 d)], \quad (31)$$

respectively, with  $\delta_0$  independent of the distance  $d$ . Notice that the above results are generalizable to the case of different dispersion relations and form factors, provided the on-shell parameters are defined as in Eq. (28). When the interatomic distance satisfies  $k_0 d = n\pi$ , with  $n$  a positive integer, the lifetime of state  $|\Psi^s\rangle$  with  $s = (-1)^{n+1}$  becomes infinite,  $\gamma_s = 0$ . On the other hand, when  $k_0 d = (n + 1/2)\pi$ , the symmetric and antisymmetric atomic excitations have the same lifetime, which is equal to that of an isolated atom. In all cases, the sum of the two decay rates is twice the decay rate of an isolated excited atom. Based on the consideration of the previous section, it is evident that the lowest-order on-shell contribution to the self-energy of  $|e_A, e_B\rangle$  reads

$$\sigma_2 = \Sigma_2^{(2)}(2\omega_0 + i0) \simeq 2\delta_0 - 4\pi i \frac{g_0^2}{c_0}, \quad (32)$$

where, as expected, the on-shell decay rate of the double excitation is twice the rate for a single atom.

## V. TWO-PHOTON CORRELATED EMISSION

Knowledge of  $A(k_1, k_2, z)$  enables one to compute, through Eqs. (24) and (9), the photon correlation function at any time  $t$ . This function will feature damped contributions, due to the cuts along the real axis on the single- and double-excitation propagators, and asymptotically stable terms, approaching, at large times (larger than the lifetimes of the excitations), the form

$$A_\infty(k_1, k_2, t) = \mathcal{A}(k_1, k_2, \omega(k_1) + \omega(k_2)) e^{-i(\omega(k_1) + \omega(k_2))t} + A_{\text{bt}}(k_1, k_2, t), \quad (33)$$

where  $\mathcal{A}$  is defined in Eq. (26) and is the dominant contribution, given by the residue of the bare two-photon pole  $z = \omega(k_1) + \omega(k_2)$  appearing in (25), while the term  $A_{\text{bt}}$  (below threshold) arises due to real poles below the branching points for the renormalized propagators and vertices, and represents a small correction in the weak-coupling regime. For instance, for the dispersion relation (27), the single-excitation propagator  $[z - \omega_0 - \omega(k) - \Sigma_+(z - \omega(k))]^{-1}$  diverges at  $z - \omega(k) = E_p$ , with

$$E_p \simeq M \left( 1 - \frac{8\pi^2 \lambda^4}{M^2(\omega_0 - M)^2} \right), \quad (34)$$

with a residue that scales like  $\lambda^4$ , while no pole below threshold is present in the propagator of the antisymmetric excitation, at least for small coupling. In the special cases in which, in the  $\mathcal{N} = 1$  sector, a bound state with energy  $E > M$  exists, it would be necessary to include an additional asymptotic contribution to (33). However, the contributions to the amplitude (26) stemming from resonant bound states are suppressed, since the peaks of the corresponding residues are compensated by the numerators  $(1 + s e^{ikd})$  that vanish at  $k = \bar{k}$  such that  $E = \omega(\bar{k})$ . From the large-time limit of the two-photon amplitude, one can also determine the two-photon spectral probability

$$P(k_1, k_2) = \lim_{t \rightarrow \infty} |A(k_1, k_2, t)|^2, \quad (35)$$

$A$  being the full two-photon amplitude (24). Notice that  $P(k_2, k_1)$  is symmetric in its arguments, due to the bosonic nature of the two-photon wave function ( $|k_1, k_2\rangle$  and  $|k_2, k_1\rangle$  represent the same state).

Before extending the numerical computation to a wider range of couplings, let us discuss the analytical results when  $\lambda \rightarrow 0$ . As the coupling vanishes, the asymptotic two-photon amplitude  $\mathcal{A}(k_1, k_2, \omega(k_1) + \omega(k_2))$  in (33) becomes concentrated around regions of linear size  $O(\lambda^2)$  around the four points  $\omega(k_1) = \omega(k_2) = \omega_0$  in the two-photon momentum space, while the additional pole contributions  $A_{\text{bs}}$  become vanishingly small. For symmetry reasons, it is enough to focus on the points  $(k_0, k_0)$  and  $(k_0, -k_0)$ , around which  $\mathcal{A}(k_1, k_2, \omega(k_1) + \omega(k_2))$  is well approximated by

$$\mathcal{A}_{\Leftrightarrow}(k_1, k_2) = \sum_{s=\pm} s(1 + s e^{ik_0 d})^2 F_s(k_1 - k_0, k_2 - k_0), \quad (36)$$

$$\mathcal{A}_{\Leftarrow\Rightarrow}(k_1, k_2) = \sum_{s=\pm} s|1 + s e^{ik_0 d}|^2 F_s(k_1 - k_0, -k_2 - k_0), \quad (37)$$

respectively, where parallel ( $\Leftrightarrow$ ) and antiparallel ( $\Leftarrow\Rightarrow$ ) arrows denote photons emitted in the same (opposite) direction, and with

$$F_s(k_1, k_2) = \frac{\lambda^2}{2\omega_0 c_0(k_1 + k_2) - \sigma_2} \times \left( \frac{1}{c_0 k_1 - \sigma_s} + \frac{1}{c_0 k_2 - \sigma_s} \right), \quad (38)$$

where  $\sigma_\pm = \delta_0 + \delta_s - i\gamma_s/2$  are defined in Eqs. (30) and (31), and  $\sigma_2$  is introduced in Eq. (32). From these results, we can obtain the following approximate expression for the asymptotic probability density (35) close to the on-shell points:

$$P(k_1, k_2) = 8 \left\{ 2 \cos^4 \left( \frac{k_0 d}{2} \right) |F_+(k_1 - k_0, \pm k_2 - k_0)|^2 + 2 \sin^4 \left( \frac{k_0 d}{2} \right) |F_-(k_1 - k_0, \pm k_2 - k_0)|^2 \pm \sin^2(k_0 d) \text{Re}[F_+^*(k_1 - k_0, \pm k_2 - k_0) \times F_-(k_1 - k_0, \pm k_2 - k_0)] \right\}, \quad (39)$$

where  $+$  and  $-$  is for photons emitted in the same (parallel) and opposite (antiparallel) directions, respectively. In the

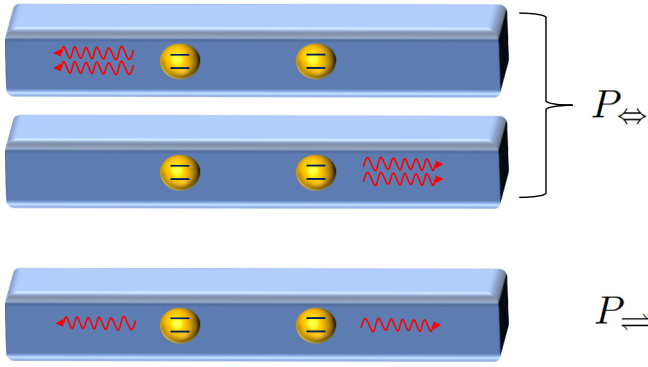


FIG. 5. Representation of the processes that contribute to the probability of parallel ( $P_{\leftrightarrow}$ ) and antiparallel ( $P_{\rightleftharpoons}$ ) photon pair emission.

limit  $\lambda \rightarrow 0$ , the integrals over the different quadrants of the  $(k_1, k_2)$  plane can be evaluated, yielding

$$\begin{aligned} P_{\leftrightarrow} &= \frac{1}{2} \int_{D_{\leftrightarrow}} dk_1 dk_2 P(k_1, k_2) \\ &= \frac{1}{2} \left( 1 + \frac{\sin^2(k_0 d)}{1 + \sin^2(k_0 d)} \right), \end{aligned} \quad (40)$$

$$\begin{aligned} P_{\rightleftharpoons} &= \frac{1}{2} \int_{D_{\rightleftharpoons}} dk_1 dk_2 P(k_1, k_2) \\ &= \frac{1}{2} \left( 1 - \frac{\sin^2(k_0 d)}{1 + \sin^2(k_0 d)} \right), \end{aligned} \quad (41)$$

where  $D_{\leftrightarrow} = \{(k_1, k_2) \in \mathbb{R}^2 | k_1 k_2 > 0\}$  and  $D_{\rightleftharpoons} = \{(k_1, k_2) \in \mathbb{R}^2 | k_1 k_2 < 0\}$ . The factor  $1/2$  has been introduced to remove redundancy with respect to momentum exchange. The processes contributing to  $P_{\leftrightarrow}$  and  $P_{\rightleftharpoons}$  are pictorially represented in Fig. 5.

The ratio of asymptotic probabilities to observe parallel and antiparallel photon pairs reads

$$R(\lambda) \Big|_{\lambda \rightarrow 0} = \frac{P_{\leftrightarrow}}{P_{\rightleftharpoons}} = 1 + 2 \sin^2(k_0 d), \quad (42)$$

being minimal and equal to 1 at resonance, when the two photons are emitted in states with the same spatial symmetry, characterized by equal weights of the parallel and antiparallel configurations. The limiting value of  $R$  is universal, in the sense that it depends only on the dimensionless product between interatomic distance and momentum of the emitted photon and not on the dispersion relation, the atomic excitation energy, or the speed of propagation. Nonetheless, it is crucially determined by the dynamics through the relation between the phase shifts and the linewidths in Eqs. (30) and (31). The maximal value  $R = 3$  corresponds to the off-resonant points  $\sin(k_0 d) = \pm 1$ , where constructive interference between photon states with opposite spatial symmetry favors parallel photon emission.

This effect is similar to the photon bunching occurring in a Hong-Ou-Mandel (HOM) interferometer [52], with the role of the input photons played by the initial double atomic excitation. In fact, neglecting dynamical effects, in the off-resonant case  $k_0 d = (n + 1/2)\pi$  the atom pair is expected

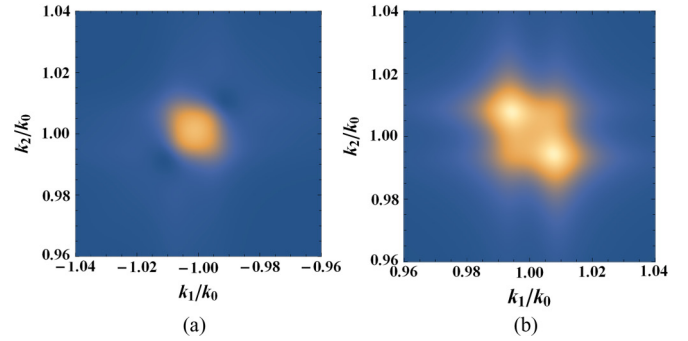
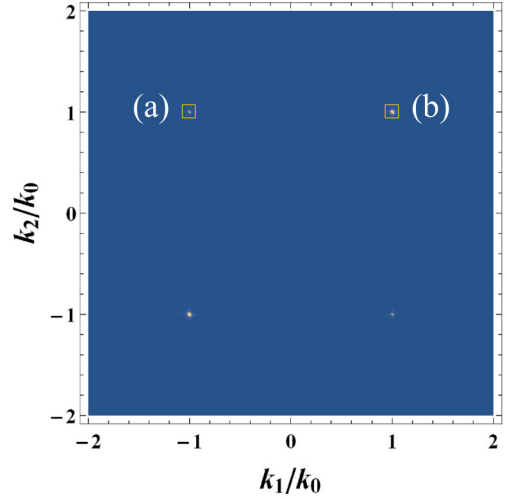


FIG. 6. The upper panel displays the density plot of the two-photon distribution  $P(k_1, k_2)$ , normalized to its maximal value, for  $\omega_0 = 1.1M$ ,  $\lambda = 10^{-2}M$ , and  $k_0 d = \pi/2$ . Colors range from blue (normalized density equal to 0) to white (normalized density equal to 1). It is evident that the probability is concentrated in very small areas of linear size  $O(\lambda^2)$  around the on-shell points. The lower panels (a) and (b) represent magnifications of the on-shell peaks highlighted in the upper plot, around  $(-k_0, k_0)$  and  $(k_0, k_0)$ , respectively. The different shape of these peaks is due to the fact that emission with intermediate symmetric and antisymmetric atomic states interfere constructively in the parallel case (b) and destructively in the antiparallel case (a). For such choice of parameters, the ratio  $R(\lambda)$  between the total parallel and antiparallel emission is close to 3.

to behave like the beam splitter in the HOM experiment, fully suppressing the possibility of antiparallel emission (i.e.,  $R \rightarrow \infty$ ). However, the two-photon emission differs from the HOM case in two aspects, both related to dynamics: first, the emitted photons are characterized by a typical momentum distribution and the relative phase between spatially symmetric and antisymmetric photons depends on momentum; second, the difference in the energy shifts  $\delta_{\pm}$  [see Eq. (30)] lifts the degeneracy between the symmetric and antisymmetric atomic excitations. The combination of such effects regularize the ratio to a nontrivial finite value, as in Eq. (42). Notice that a different expression of  $\delta_{\pm}$  and  $\gamma_{\pm}$  would lead to generally different value of  $R$ . The effect of interference between symmetric and antisymmetric states on the structure of the parallel and antiparallel peaks is displayed in Fig. 6.

In order to compute the two-photon amplitude in the case of larger couplings, some approximations are needed. In

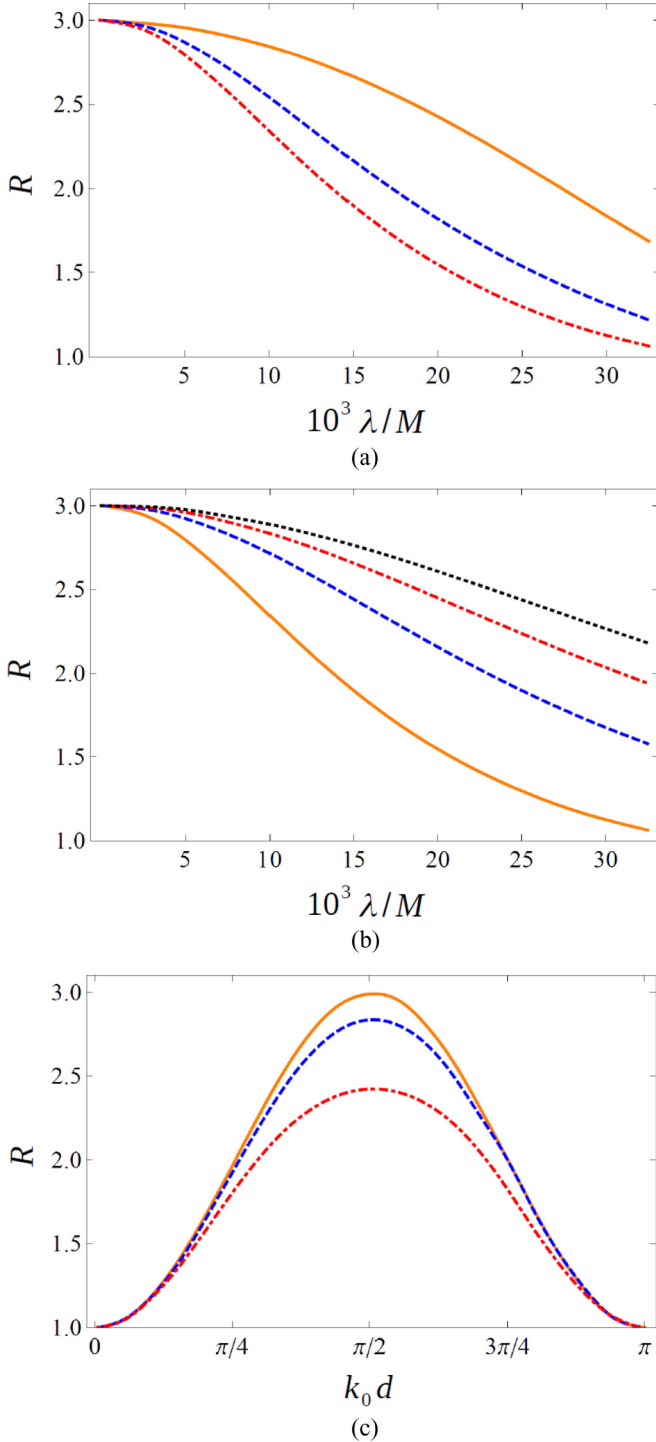


FIG. 7. Plots of the ratio  $R = P_{\leftrightarrow}/P_{\rightleftharpoons}$  in different conditions. Panel (a): Dependence of  $R$  on  $\lambda$  at fixed  $\omega_0 = 1.1M$ , for  $d = \pi/(2k_0)$  (solid orange line),  $d = 3\pi/(2k_0)$  (dashed blue line), and  $d = 5\pi/(2k_0)$  (dot-dashed red line). Panel (b): Dependence of  $R$  on  $\lambda$  in the case  $d = 5\pi/(2k_0)$  for  $\omega_0 = 1.1M$  (solid orange line),  $\omega_0 = 1.2M$  (dashed blue line),  $\omega_0 = 1.3M$  (red dot-dashed line), and  $\omega_0 = 1.4M$  (dotted black line). Panel (c): Dependence of  $R$  on  $k_0 d$ , at fixed  $\omega_0 = 1.1M$ , for  $\lambda = 10^{-3}M$  (solid orange line),  $\lambda = 10^{-2}M$  (dashed blue line), and  $\lambda = 2 \times 10^{-2}M$  (red dot-dashed line).

particular, it is not possible to express the vertices  $X_s(k, z)$ , defined in Eq. (21) and represented in Fig. 3, in a closed form.

We choose to truncate the expansion of  $X_s$  at the first diagram, thereby regularizing the intermediate single-excitation propagator with its on-shell self-energy  $\sigma_s = \Sigma(\omega_0 + i0)$ . Namely, we approximate the vertex corrections as

$$\begin{aligned} X_s(k, z) &\simeq \int dq \frac{g^2(q)(1 + s \cos(qd))}{(z - \omega(k) - \omega(q))(z - \omega_0 - \omega(q) - \sigma_s)} \\ &= \frac{\Sigma_s(z - \omega_0 - \sigma_s) - \Sigma_s(z - \omega(k))}{\omega_0 + \sigma_s - \omega(k)}. \end{aligned} \quad (43)$$

Some relevant results are displayed in Fig. 7. In general, the plots show that  $R(\lambda)$  is a decreasing function of the coupling strength, and the effects of increasing the coupling are more relevant in the off-resonance cases [ $k_0 d = (n + 1/2)\pi$ ]. However, if one considers  $d \in [(n - 1/2)\pi/k_0, (n + 1/2)\pi/k_0]$ ,  $R$  remains an increasing function of the distance  $|d - n\pi/k_0|$  from the resonance value. The decrease of  $R$  with  $\lambda$  is mitigated by the discrepancy of the excitation energy  $\omega_0$  with respect to the propagation cutoff  $M$ , and enhanced by the distance  $d$ , if one considers the cases  $k_0 d = (n + \alpha)\pi$  with  $\alpha$  real and fixed. These effects are due to a different behavior of the peak widths in the parallel and antiparallel cases, and to the emergence of strong-coupling effects due to the poles below threshold, which are correctly taken into account in the computation. Since the distance, the coupling strength, and the excitation energy are fully independent parameters, the results suggest that correlated two-photon emission in a linear waveguide can be possibly used to determine one of them when the other two are known. In particular, in the small-coupling regime, the relation (42) depends only on a relation between  $d$  and  $\omega_0$ .

## VI. CONCLUSIONS AND OUTLOOK

We explored the physics of a pair of two-level atoms, coupled to a 1D waveguide mode, in the double-excitation sector. In particular, we investigated the properties of correlated photon emission, that are drastically affected by interatomic distance, and are also influenced by the strength of interaction. We obtained analytical results in the small-coupling regime, showing that the relative probability of parallel emission with respect to the antiparallel case is determined by dynamical quantities.

The experimental measurement of correlations can be exploited to detect properties of the atomic pair, such as their distance, the strength of interactions with the waveguide field, asymmetries in their excitation frequency, and other kinds of impurities. The initial state, in which both atoms are excited, can be prepared by a scattering process in which a photon wave packet shines the atoms. This requires additional frequencies and a time analysis of the excitation process and population transfer between the two atoms. An alternative protocol would be available if a third level  $|f\rangle$  of each atom was accessible such that the transitions  $f \leftrightarrow e$  and  $f \leftrightarrow g$  were not coupled to the waveguide field. The existence of

a fast transition from  $|f\rangle$  to  $|e\rangle$  would make possible a population inversion by pumping the system from  $|g\rangle$  to  $|f\rangle$  with an external field. Further research will be devoted to the investigation of the effects of the two-excitation dynamics on one- and two-photon scattering and stimulated emission by the atomic pair. Moreover, the predicted directionality of the emissions suggests the possibility that the system here analyzed can act as a quantum optical diode [53].

## ACKNOWLEDGMENTS

We thank Tommaso Tufarelli, Myungshik S. Kim, and Francesco Ciccarello for discussions. P.F., S.P., and D.P. are partially supported by Istituto Nazionale di Fisica Nucleare (INFN) through the project “QUANTUM.” F.V.P. is supported by INFN through the project “PICS.” P.F. is partially supported by the Italian National Group of Mathematical Physics (GNFM-INdAM).

- 
- [1] T. Giamarchi, *Quantum Physics in One Dimension* (Oxford University Press, Oxford, 2004).
- [2] Y. Kuramoto and Y. Kato, *Dynamics of One-Dimensional Quantum Systems: Inverse-Square Interaction Models* (Cambridge University Press, Cambridge, UK, 2009).
- [3] C. Cohen-Tannoudji, J. Dupont-Roc, and G. Grynberg, *Atom-Photon Interactions: Basic Processes and Applications* (Wiley-VCH Verlag GmbH, Weinheim, Germany, 1998).
- [4] J. M. Raimond, M. Brune, and S. Haroche, Manipulating quantum entanglement with atoms and photons in a cavity, *Rev. Mod. Phys.* **73**, 565 (2001).
- [5] *Cavity Quantum Electrodynamics, Advances in Atomic, Molecular & Optical Physics*, 1st ed., edited by P. R. Berman, D. R. Bates, and B. Bederson (Academic Press, Boston, MA, 1994).
- [6] E. A. Hinds, Cavity quantum electrodynamics, *Adv. At. Mol. Opt. Phys.* **28**, 237 (1990).
- [7] S. Haroche, in *Fundamental Systems in Quantum Optics*, Proceedings of the Les Houches Summer School of Theoretical Physics, edited by J. Dalibard, J.-M. Raimond, and J. Zinn-Justin (North-Holland, Amsterdam, 1992), p. 767.
- [8] A. Blais, R.-S. Huang, A. Wallraff, S. M. Girvin, and R. J. Schoelkopf, Cavity quantum electrodynamics for superconducting electrical circuits: An architecture for quantum computation, *Phys. Rev. A* **69**, 062320 (2004).
- [9] J. Q. You and F. Nori, Atomic physics and quantum optics using superconducting circuits, *Nature (London)* **474**, 589 (2011).
- [10] E. Vetsch, D. Reitz, G. Sague, R. Schmidt, S. T. Dawkins, and A. Rauschenbeutel, Optical Interface Created by Laser-Cooled Atoms Trapped in the Evanescent Field Surrounding an Optical Nanofiber, *Phys. Rev. Lett.* **104**, 203603 (2010).
- [11] M. Bajcsy, S. Hofferberth, V. Balic, T. Peyronel, M. Hafezi, A. S. Zibrov, V. Vuletic, and M. D. Lukin, Efficient All-Optical Switching Using Slow Light within a Hollow Fiber, *Phys. Rev. Lett.* **102**, 203902 (2009).
- [12] U. Dorner and P. Zoller, Laser-driven atoms in half-cavities, *Phys. Rev. A* **66**, 023816 (2002).
- [13] G. Zumofen, N. M. Mojarad, V. Sandoghdar, and M. Agio, Perfect Reflection of Light by an Oscillating Dipole, *Phys. Rev. Lett.* **101**, 180404 (2008).
- [14] N. Lindlein, R. Maiwald, H. Konermann, M. Sondermann, U. Peschel, and G. Leuchs, A new  $4\pi$  geometry optimized for focusing on an atom with a dipolelike radiation pattern, *Laser Phys.* **17**, 927 (2007).
- [15] A. Wallraff, D. I. Schuster, A. Blais, L. Frunzio, R.-S. Huang, J. Majer, S. Kumar, S. M. Girvin, and R. J. Schoelkopf, Strong coupling of a single photon to a superconducting qubit using circuit quantum electrodynamics, *Nature (London)* **431**, 162 (2004).
- [16] O. Astafiev, A. M. Zagoskin, A. A. Abdumalikov, Jr., Yu. A. Pashkin, T. Yamamoto, K. Inomata, Y. Nakamura, and J. S. Tsai, Resonance fluorescence of a single artificial atom, *Science* **327**, 840 (2010).
- [17] I.-C. Hoi, A. F. Kockum, L. Tornberg, A. Pourkabirian, G. Johansson, P. Delsing, and C. M. Wilson, Probing the quantum vacuum with an artificial atom in front of a mirror, *Nat. Phys.* **11**, 1045 (2015).
- [18] H. Dong, Z. R. Gong, H. Ian, L. Zhou, and C. P. Sun, Intrinsic cavity QED and emergent quasinormal modes for a single photon, *Phys. Rev. A* **79**, 063847 (2009).
- [19] T. Tufarelli, F. Ciccarello, and M. S. Kim, Dynamics of spontaneous emission in a single-end photonic waveguide, *Phys. Rev. A* **87**, 013820 (2013).
- [20] J.-T. Shen and S. Fan, Coherent Single Photon Transport in a One-Dimensional Waveguide Coupled with Superconducting Quantum Bits, *Phys. Rev. Lett.* **95**, 213001 (2005).
- [21] A. Faraon, E. Waks, D. Englund, I. Fushman, and J. Vučković, Efficient photonic crystal cavity-waveguide couplers, *Appl. Phys. Lett.* **90**, 073102 (2007).
- [22] B. Dayan, A. S. Parkins, Takao Aoki, E. P. Ostby, K. J. Vahala, and H. J. Kimble, A photon turnstile dynamically regulated by one atom, *Science* **319**, 1062 (2008).
- [23] J. S. Douglas, H. Habibian, C.-L. Hung, A. V. Gorshkov, H. J. Kimble, and D. E. Chang, Quantum many-body models with cold atoms coupled to photonic crystals, *Nat. Photonics* **9**, 326 (2015).
- [24] A. Goban, C.-L. Hung, J. D. Hood, S.-P. Yu, J. A. Muniz, O. Painter, H. J. Kimble, Superradiance for Atoms Trapped along a Photonic Crystal Waveguide, *Phys. Rev. Lett.* **115**, 063601 (2015).
- [25] A. González-Tudela, V. Paulisch, H. J. Kimble, and J. I. Cirac, Efficient Multiphoton Generation in Waveguide Quantum Electrodynamics, *Phys. Rev. Lett.* **118**, 213601 (2017).
- [26] J. Bleuse, J. Claudon, M. Creasey, N. S. Malik, J.-M. Gérard, I. Maksymov, J.-P. Hugonin, and P. Lalanne, Inhibition, Enhancement, and Control of Spontaneous Emission in Photonic Nanowires, *Phys. Rev. Lett.* **106**, 103601 (2011).
- [27] M. E. Reimer, G. Bulgarini, N. Akopian, M. Hocevar, M. B. Bavinck, M. A. Verheijen, E. P. A. M. Bakkers, L. P. Kouwenhoven, and V. Zwiller, Bright single-photon sources in bottom-up tailored nanowires, *Nat. Commun.* **3**, 737 (2012).
- [28] T. Shi, D. E. Chang, and J. I. Cirac, Multiphoton-scattering theory and generalized master equations, *Phys. Rev. A* **92**, 053834 (2015).
- [29] T. Shi, Y.-H. Wu, A. Gonzalez-Tudela, J. I. Cirac, Bound States in Boson Impurity Models, *Phys. Rev. X* **6**, 021027 (2016).



- [30] E. Sanchez-Burillo, D. Zueco, L. Martin-Moreno, J. J. Garcia-Ripoll, Dynamical signatures of bound states in waveguide QED, *Phys. Rev. A* **96**, 023831 (2017).
- [31] K. Lalumière, B. C. Sanders, A. F. van Loo, A. Fedorov, A. Wallraff, and A. Blais, Input-output theory for waveguide QED with an ensemble of inhomogeneous atoms, *Phys. Rev. A* **88**, 043806 (2013).
- [32] D. Witthaut and A. S. Sørensen, Photon scattering by a three-level emitter in a one-dimensional waveguide, *New J. Phys.* **12**, 043052 (2010).
- [33] A. Gonzalez-Tudela, D. Martin-Cano, E. Moreno, L. Martin-Moreno, C. Tejedor, and F. J. Garcia-Vidal, Entanglement of Two Qubits Mediated by One-Dimensional Plasmonic Waveguides, *Phys. Rev. Lett.* **106**, 020501 (2011).
- [34] E. Shahmoon and G. Kurizki, Nonradiative interaction and entanglement between distant atoms, *Phys. Rev. A* **87**, 033831 (2013).
- [35] P. Facchi, M. S. Kim, S. Pascazio, F. V. Pepe, D. Pomarico, and T. Tufarelli, Bound states and entanglement generation in waveguide quantum electrodynamics, *Phys. Rev. A* **94**, 043839 (2016).
- [36] P. Facchi, S. Pascazio, F. V. Pepe, and K. Yuasa, Long-lived entanglement of two multilevel atoms in a waveguide, *J. Phys. Commun.* **2**, 035006 (2018).
- [37] X. H. H. Zhang and H. U. Baranger, Heralded Bell state of 1D dissipative qubits using classical light, [arXiv:1809.00685](https://arxiv.org/abs/1809.00685).
- [38] H. Zheng and H. U. Baranger, Persistent Quantum Beats and Long-Distance Entanglement from Waveguide-Mediated Interactions, *Phys. Rev. Lett.* **110**, 113601 (2013).
- [39] C. Gonzalez-Ballester, F. J. Garcia-Vidal, and E. Moreno, Non-Markovian effects in waveguide-mediated entanglement, *New J. Phys.* **15**, 073015 (2013).
- [40] E. S. Redchenko and V. I. Yudson, Decay of metastable excited states of two qubits in a waveguide, *Phys. Rev. A* **90**, 063829 (2014).
- [41] M. Laakso and M. Pletyukhov, Scattering of Two Photons from Two Distant Qubits: Exact Solution, *Phys. Rev. Lett.* **113**, 183601 (2014).
- [42] H. Pichler and P. Zoller, Photonic Circuits with Time Delays and Quantum Feedback, *Phys. Rev. Lett.* **116**, 093601 (2016).
- [43] A. F. van Loo, A. Fedorov, K. Lalumière, B. C. Sanders, A. Blais, and A. Wallraff, Photon-mediated interactions between distant artificial atoms, *Science* **342**, 1494 (2013).
- [44] V. I. Yudson, Dynamics of the integrable one-dimensional system “photons + two-level atoms,” *Phys. Lett. A* **129**, 17 (1988).
- [45] V. I. Yudson and P. Reineker, Multiphoton scattering in a one-dimensional waveguide with resonant atoms, *Phys. Rev. A* **78**, 052713 (2008).
- [46] Yao-Lung L. Fang and H. U. Baranger, Waveguide QED: Power spectra and correlations of two photons scattered off multiple distant qubits and a mirror, *Phys. Rev. A* **91**, 053845 (2015).
- [47] T. S. Tsoi and C. K. Law, Quantum interference effects of a single photon interacting with an atomic chain inside a one-dimensional waveguide, *Phys. Rev. A* **78**, 063832 (2008).
- [48] T. Ramos, B. Vermersch, P. Hauke, H. Pichler, and P. Zoller, Non-Markovian dynamics in chiral quantum networks with spins and photons, *Phys. Rev. A* **93**, 062104 (2016).
- [49] R. H. Dicke, Coherence in spontaneous radiation processes, *Phys. Rev.* **93**, 99 (1954).
- [50] M. Gross and S. Haroche, Superradiance: An essay on the theory of collective spontaneous emission, *Phys. Rep.* **93**, 301 (1982).
- [51] J. D. Jackson, *Classical Electrodynamics* (John Wiley & Sons, New York, 1999).
- [52] C. K. Hong, Z. Y. Ou, and L. Mandel, Measurement of Subpicosecond Time Intervals Between Two Photons by Interference, *Phys. Rev. Lett.* **59**, 2044 (1987).
- [53] A. Rosario Hamann, C. Müller, M. Jerger, M. Zanner, J. Combes, M. Pletyukhov, M. Weides, T. M. Stace, and A. Fedorov, Nonreciprocity Realized with Quantum Nonlinearity, *Phys. Rev. Lett.* **121**, 123601 (2018).